World Conference on Timber Engineering Oslo 2023

MASS TIMBER BRACED FRAMES WITH MASS TIMBER BUCKLING RESTRAINED BRACES

Emily Wiliamson[1], Chris P. Pantelides[2], Hans-Erik Blomgren[3], Douglas Rammer[4]

ABSTRACT: A mass timber lateral force resisting system (LFRS) is proposed using a timber buckling restrained brace (TBRB) for improved seismic performance in high seismic applications. To develop a high-performance braced frame, it is essential to quantify the behaviour of the connections including failure modes and moment-rotation capacities. Cyclic and monotonic tests were conducted on six mass timber beam-column connections to investigate the response of mass timber joints connected with slotted-in steel plates and mild steel dowels. The goal of the subassembly tests was to measure the maximum rotation of such connections for monotonic and cyclic loads; these results were used to optimize the number of mild steel dowels for the TBRB frame design. The tests showed that the connections with three different steel dowel details reached a maximum rotation of 0.11 rad. with no loss of strength. Scaled tests of a full braced timber frame with a TBRB were carried out to verify the LFRS which included the effect of column axial load and out-of-plane displacements.

KEYWORDS: Braced frame, Buckling restrained brace, Lateral Force resisting system, Mass timber, Seismic

1 INTRODUCTION

Mass timber buildings are popular due to their sustainable characteristics, architectural appeal, and high strength-to-weight ratio. Engineered timber products such as glulam, cross laminated timber (CLT) and mass ply panels (MPP) allow engineers to take advantage of these characteristics. Currently, tall timber buildings must be combined with a lateral force resisting system (LFRS) made of steel or reinforced concrete because current building codes lack defined values for a ductile timber LFRS; this can lead to compatibility issues and increase construction cost and time.

A ductile timber (LFRS) is needed for the expanded use of mass timber in new taller buildings. There has been some work to develop and improve the performance of CLT shear walls [1-6], but shear wall systems can limit the flexibility of the building floor plan. Current timber frames have limited hysteretic energy dissipation and ductility capabilities because they rely on the connections for the response to loading [7-8]. To address this issue, researchers have developed a buckling restrained brace with a timber casing (TBRB) [9]; tests showed that a TBRB exceeds the qualification requirements of a conventional BRB [10]. Researchers have also completed a series of TBRB tests to propose new design methods and avoid certain failure modes such as bulging of the timber restraining element [11]. Furthermore, researchers have successfully tested a full-scale glulam frame with two conventional steel and concrete BRBs in a chevron configuration [12].

The overall performance of a complete TBRB frame (TBRBF) also depends on the beam-column and gusset plate connection performance. Researchers have been interested in the performance of moment resisting timber connections for some time [13-16]; however, dowel-type connections often experience premature failure due to tension splitting of the timber under induced beam-column joint rotations. Additional reinforcement perpendicular to the grain is often required to improve connection performance. Joint reinforcement with screws placed perpendicular to grain using glulam connections achieved a maximum rotation of 0.08 radians [17]. Dowels arranged in a circular pattern using plywood as reinforcing for the joints achieved a maximum rotation of 0.03 radians [18].

In this study, six beam-column joints were designed and tested under monotonic and cyclic loads with varying number of dowels. Mass ply lam (MPL) [19] was used for the beams and columns to provide resistance against perpendicular-to-grain tension splitting in the connection regions due to the additional strength and stiffness provided by the cross-ply veneers included the layup of the material. Informed by the results of the beam-column connection tests, an MPL frame with a TBRB was designed and tested. The frame was tested with multiple levels of axial force applied to the columns and with some out-of-plane displacement imposed on the frame. In addition to the TBRBF subassembly tests, the frame was tested on its own to monitor the condition of the connections and provide an improved understanding on the TBRB contribution to the performance of the subassembly.

[1] Res. Assist., Dept. of Civil and Env. Eng., University of Utah, USA, emily.diedrich@utah.edu
[2] Prof., Dept. of Civil and Env. Eng., University of Utah, USA, c.pantelides@utah.edu
[3] Struct. Eng., Timberlab, USA, h.blomgren@timberlab.com
[4] Res. Eng., Forest Products Laboratory, USA, douglas.r.rammer@usda.gov

https://doi.org/10.52202/069179-0265

2 MASS TIMBER CONNECTION TESTS

The initial phase of the research discussed in this paper includes the design and testing of six beam-column connections [20]. These tests were carried out to provide a clearer understanding of the connection performance including failure modes, moment-rotation relationships and rotation capacity.

2.1 CONNECTION EXPERIMENT DESIGN

The connections designed for the experimental program were meant to represent a beam-column-brace connection within a TBRBF with a beam span of 4.27 m and a story height of 2.90 m (Figure 1). The length of the members was based on cutting the joint out at the mid-span of the beam and at half a story height above and below the joint. The beam and column were 381 mm square MPL, a material made of layers of laminated veneer lumber with different cross grain directions of the veneer layers [19]. MPL in the joist orientation (Figure 2a) was chosen to take advantage of the cross-ply layers in the layup which act as self-reinforcing and attempt to avoid the additional joint reinforcing that is typically required to improve the strength and rotation capabilities of timber connections. The members were connected with 248 MPa, 12.7 mm slotted-in steel plates and 12.7 mm diameter smooth-shank mild-steel dowels (Figure 2). In a beam-column-brace connection, the steel connection plates will extend beyond the timber members to form gusset plates for the TBRB connection, but these were not included in the connection tests. The impact of the gusset plates and brace connection on the performance of the connection was studied in more detail during the MTRBF tests described in Section 3.

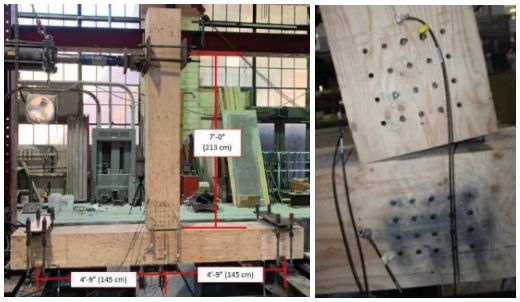

Figure 1: *Beam-column joint setup and maximum rotation for joint with 12 beam dowels*

The connections were designed to resist the overstrength forces from a 267 kN tensile yield strength TBRB using the National Design Specification (NDS) for Wood Construction and the NDS Technical Report 12 for dowel-type connectors [21,22]. The joint was idealized as an equivalent series of three-member connections [23] and the theoretical moment capacity was calculated using the model in [18]. The geometry of the dowel connection was selected to allow yield mode IV to be the limiting yield mode of the design because it is a more ductile yield mode as it is limited by the bending of the steel dowels rather than the crushing of the timber. A 25 mm gap between the end of the beam and the face of the column was built into the connection to allow for large beam rotations without contact with the column.

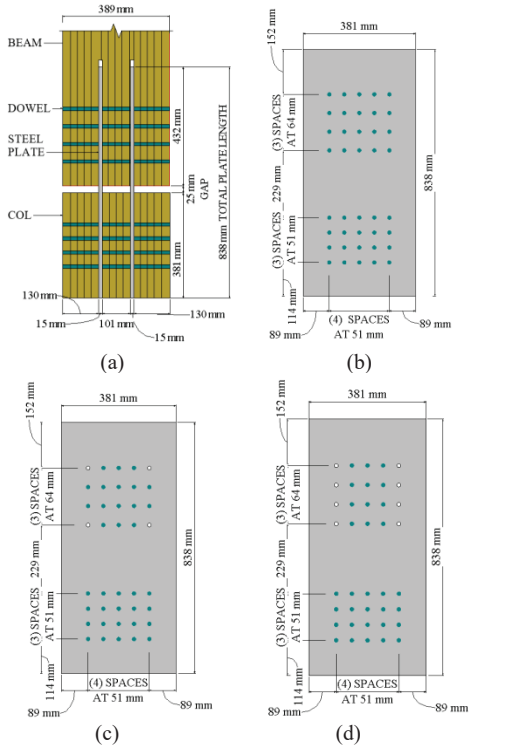

Figure 2: *Connection:(a) section, (b) 20 dowels, (c) 16 dowels, (d) 12 dowels*

Three pairs of connections were tested, each with a different number of dowels in the beam; the first pair had 20 dowels, the second pair 16, and the third pair 12. All connections had 20 column dowels. For each variation, one connection was tested under monotonic loading and one under cyclic loading. The cyclic loading protocol was adopted from ASTM E2126 test method B [24]; the loading protocol was defined with the maximum horizontal displacement imposed on the beam end as 254 mm, which was equivalent to the maximum stroke of the actuator used to apply the load (Figure 3). To facilitate testing, the joint was rotated 90 degrees counter-clockwise so that the 2.13 m beam was vertical; a horizontal load was applied at the beam end (Figure 1).

https://doi.org/10.52202/069179-0265

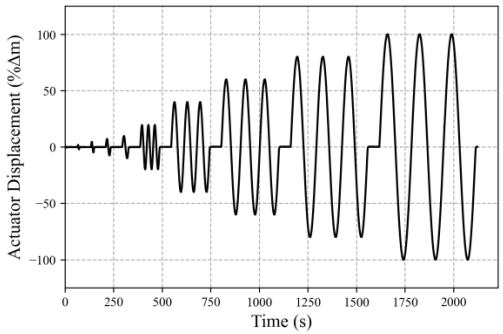

***Figure 3**: ASTM E2126 test method B loading protocol*

2.2 CONNECTION EXPERIMENTAL RESULTS

All six joints reached a maximum rotation of 0.11 radians without any loss of strength or any visible external damage such as timber splitting in the joint region; the only joint that experienced contact between the beam and column was the joint with 12 dowels in the beam under monotonic loading (Figure 2). The tests were stopped at 0.11 radians of rotation because this was the maximum displacement allowed by the length of the actuator. After testing was complete, the joints were dissected to observe the internal damage to the connection. Although most of the deformation observed was small, the most deformation was observed in the joint with 12 dowels in the beam (Figure 4a). In all tests, the dowels yielded in mode IV as expected based on the design; necking of dowels at the steel plate interface and elongation of the holes in the direction of the force in the respective dowel were observed (Figure 4b). Furthermore, most of the damage was observed in the dowels in the perimeter of the connection.

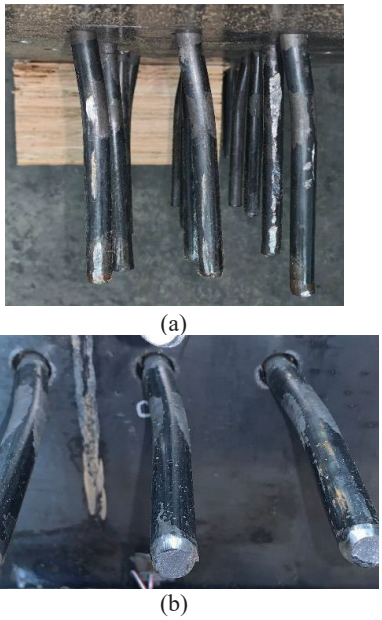

(a)

(b)

***Figure 4:** Post-test connection dissection (a)bending of the dowels and (b) deformation of the holes in the steel plate*

The moment capacity of the beam-column connections appeared to be proportional to the number of dowels in the beam (Figure 5). The envelope response of these connections can be broken down into three main stages (Figure 5a): the slip stage, the elastic stage, and post-yield stage. The second increase in load exhibited in the 12 beam dowel connection's monotonic response was caused by the contact between the beam and column, which occurred at approximately 0.09 radians. The slip stage occurs in the beginning of the loading because some displacement must be imposed on the connection before it is fully engaged. This is largely due to construction tolerances of the holes, which need to be slightly oversized in order to fit the dowel through the three timber and two steel elements. Once the dowel has overcome the gap and fully engaged with the timber, the connection is able to develop more stiffness and it enters the elastic stage. During this stage, the connection continues to develop strength until the steel dowels begin to yield. After the dowels yield and begin to deform, the connection is not able to resist additional load; however, the connection continues to rotate, resulting in a ductile connection response. The Y and K method [25] was used to estimate the yield point of the connection. The displacement ductility of these connections was then determined to range from 1.8 to 4.1 based on the maximum rotation achieve during testing; however, this is a lower bound because the tests were forced to terminate before a loss in strength occurred due to the limited stroke length of the actuator.

The hysteresis of the cyclic tests (Figure 5b) displays some pinching effects. This is common for timber doweled connections because there is some slack in the connection when the load is reversed and the dowel has some distance to recover before it is fully engaged with the timber again since it may have already crushed it in that region during a previous cycle.

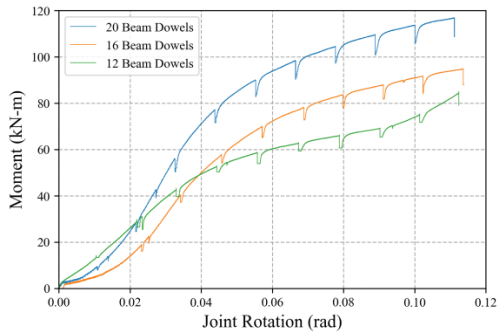

(a)

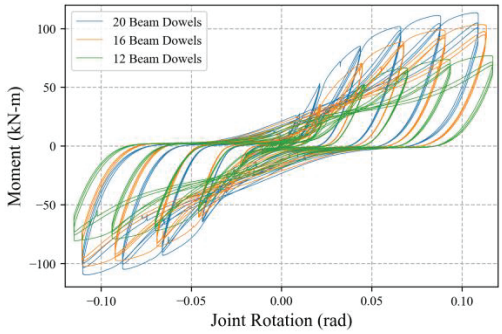

(b)

Figure 5: *Experimental results: (a) monotonic tests and (b) cyclic tests*

3 TBRBF SUBASSEMBLY TESTS

After evaluating the response of the connections during the connection tests, a TBRBF was designed and constructed for performing cyclic, quasi-static subassembly tests (Figure 6).

3.1 TBRBRF SUBASSEMBY EXPERIMENT DESIGN

The frame was designed as an approximately two-thirds scale, single-bay frame with a column spacing of 3.05 m and a story height of 2.29 m. To properly simulate the performance of a frame in an upper story of a building, the columns were extended beyond the bottom beam to the strong floor. Furthermore, the base of the west column was designed to be a roller to drag the horizontal component of the brace force through the bottom beam to the base of the east column, which was fixed by extending the connection plates 25 mm lower than the base of the column and welding it to the steel support structure. The beams and columns are of the same MPL material and same cross-section as the joint tests described in Section 2. The connections in the frame also have two 12.7 mm thick slotted-in steel plates and are connected by 12.7 mm diameter mild steel dowels. All connections were designed using the same approach as described in Section 2.1 of this paper for the expected forces of a TBRB with a tensile yield force of 178 kN. The expected forces were determined with a compression adjustment factor of 1.25 and a strain hardening factor of 1.45, which were the maximum of each value determined in [9]. The gusset plates are formed by extending the connection plates beyond the timber members; they were reinforced with steel stiffeners and steel cheek plates to ensure the TBRB would be the limiting structural element in the frame. The 25 mm gap between the beam end and column face was also implemented for the connections in the frame.

The restraining element of the TBRB is mass plywood panel (MPP) blocks bolted together on either side of the mild steel yielding core. The MPP blocks were 254 mm wide by 152 mm deep; they were placed so that the laminas were perpendicular to the steel yielding core. To achieve a 178 kN TBRB, the yielding portion of the core was specified to be 13 mm thick by 51 mm wide and have a yield stress of 276 MPa. At the ends of the brace, the core width increases to 178 mm for the pin connection to the two gusset plates. In addition, there are stiffeners welded to the ends of the core to ensure that yielding occurs within the intended yielding zone. Finally, there was a 25 mm diameter dowel welded to the steel core at the midpoint of the yielding zone to promote even load distribution and help keep the core in place within the casing. The TBRBs used in this experimental program had a pin to pin length of 2730 mm and a yielding length of 1554 mm.

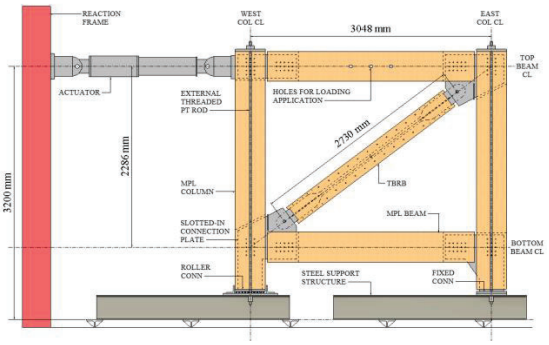

Figure 6: *Experiment of TBRBF*

The same timber frame was used for nine total tests: four TBRBF tests and five bare frame tests. The bare frame tests were done at the beginning of the testing series, at the end of the testing series, and between each TBRBF test. Moreover, the bare frame tests were completed within the elastic range of the frame to provide an understanding of the frame contribution to the subassembly performance and to monitor the condition of the connections after a TBRBF test. Two levels of axial force were applied to the columns during testing: the low-level axial load was equivalent to 5% of the column capacity and the high axial load was equivalent to 12% of the column capacity. The axial force was applied to the columns with two all-thread bars, which were external to the columns and post-tensioned to achieve the desired load level. Each level of axial load was tested once in-plane and once with a 25 mm out-of-plane displacement imposed on the top east connection. A summary of the tests is listed in Table 1.

https://doi.org/10.52202/069179-0265

Similar to the connection tests, the loading protocol adopted for these tests was based on ASTM E2126 test method B [24] (Figure 3). The cycles were defined based on a maximum displacement associated with a drift ratio of approximately 3%. To ensure the connections remained elastic during the bare frame tests, the loading protocol was terminated after the $0.6\Delta_m$ loading step.

Table 1: *Timber Frame Experimental Program*

Test Name	Out-of-plane displacement	Axial Load Level
Bare Frame	None	Low
I-TBRB1	None	Low
I-TBRB2	None	High
O-TBRB3	25 mm	Low
O-TBRB4	25 mm	High

3.2 TBRBF SUBASSEMBLY RESULTS

Frame tests without a TBRB were completed as intermediate steps during the experimental program to monitor the condition of the connections and provide insight into how the TBRBF performance compares to the bare frame performance. The hysteresis in Figure 7 is representative of all the bare frame tests that were conducted throughout the testing series since the connections experienced minimal damage during both the bare frame tests and the TBRBF tests. Because they were carried out as intermediate steps, the tests were concluded earlier in the loading protocol to ensure the connection remained mostly elastic; the slender hysteresis loops and no significant excessive drift at zero force confirm this assumption.

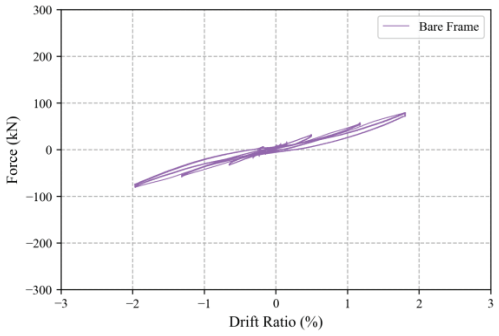

Figure 7: *Bare frame hysteresis*

The hysteresis curves for the TBRBF tests are shown in Figure 8; Figure 8a shows the response of the frames with low axial force applied to the columns and Figure 8b shows the response of the frames with high axial load. Both the level of axial load and the intentional out-of-plane displacement had little impact on the performance of the subassembly. There is a slight decrease in stiffness between the first TBRBF test, I-TBRB1, and the subsequent tests due to the slight crushing of the timber in the dowel regions caused by the first test. Some slip can be observed when the load was reversed; this is due to the movement of the dowels within their respective holes before the dowels are fully engaged. The TBRBF tests were able to achieve similar forces in tension and compression as expected from a BRB system. Furthermore, at the same drift ratio, the TBRBF resisted 3.0 to 3.8 times the amount of lateral load than the bare frame.

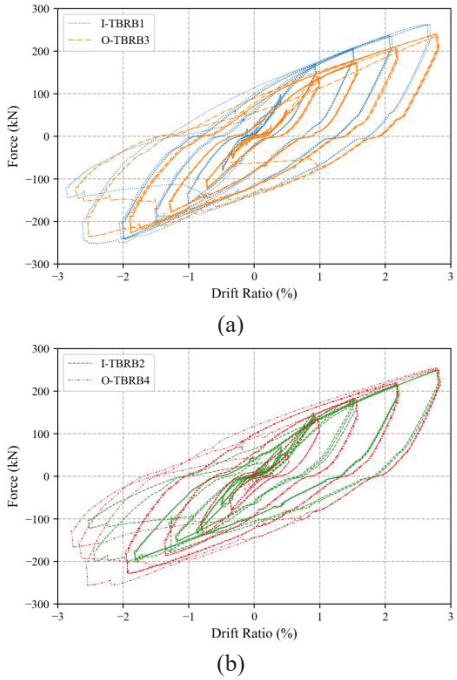

Figure 8: *TBRBF Hysteresis curves (a) low axial load and (b) high axial load*

All four of the hysteresis curves are relatively stable with minimal pinching. This indicates effective hysteretic energy dissipation (Figure 9) from the diagonal TBRB core plate. Test O-TBRB4 shows the most energy dissipation because it was allowed to complete the entire loading protocol despite TBRB failure. This shows that the system is able to continue to dissipate energy even after TBRB failure. Test I-TBRB2 dissipated the least amount of energy of the TBRBF tests because a weld in the support structure fractured during the test which caused the east column to behave as a rocking column and limited the amount of force the system was able to resist when the actuator was pulling the frame to the west (negative drift ratio). Figure 9 demonstrates the impact of the TBRB on the subassembly's ability to dissipate energy effectively. When comparing the energy dissipated by the TBRBF to the energy dissipated by the bare frame after the same number of cycles, the TBRBF dissipates 4.0 to 8.6 times the hysteretic energy dissipated by the bare frame.

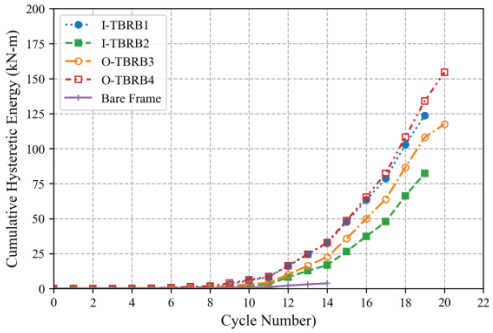

Figure 9: *Cumulative hysteretic energy*

The secant stiffness was calculated for each cycle to show the stiffness degradation of the system throughout the loading protocol. It was calculated based on the peak forces and displacements achieved for each cycle. Figure 10 shows a comparison between the stiffness of test I-TBRB1 and the first bare frame test. Since the connections provide limited moment-resisting capabilities, the stiffness of the bare frame is smaller than the stiffness of the TBRBF.

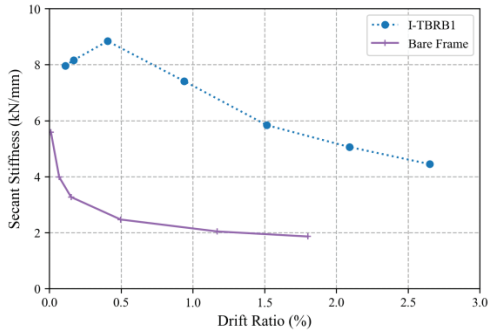

Figure 10: *Stiffness comparison between TBRBF and bare frame*

In addition to the hysteretic energy and the stiffness degradation, the ductility of the TBRBF system was evaluated using the Y and K method [25] because it is able to effectively estimate the yield point of a timber structure even when the connections have a lower initial stiffness consistent with what is observed with the dowel-type connections [26]. The maximum displacement ductility for the TBRBF tests determined by the Y and K method ranged from 3.1 to 3.5. To properly compare to existing research, the yield point and ductility was also estimated using the EEEP method [24]; the maximum displacement ductility determined by this method ranged from 2.1 to 2.9. This is double the ductility found for conventional timber brace frames [27], and comparable to the findings of research in which timber frames were tested with conventional steel-concrete BRBs [12].

All TBRBF tests experienced failure of the TBRB during the compression segment of the second cycle of the 100%Δ_m loading step. The failure was initiated by weak axis buckling of the steel core near the end of the yielding zone (Figure 11a). As the amplitude of the buckled core increased with higher displacement cycles, the casing began to split between the layers at the location of the largest wave; the splitting eventually propagated along the length of the casing (Figure 11b)

(a)

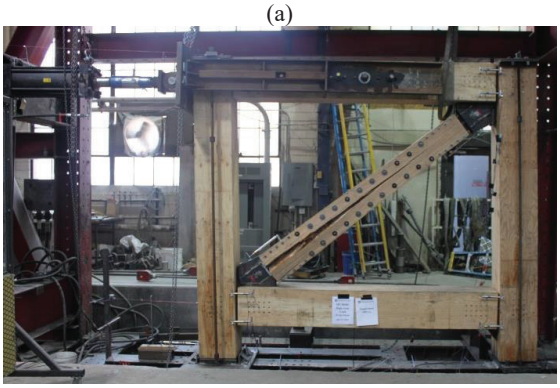

(b)

Figure 11: *TBRB failure modes (a) weak axis buckling of the steel cores and (b) splitting of the MPP casing*

The connections of the timber frame experienced no visible external damage such as tension splitting or timber crushing. After the testing series was complete, the connections were dissected to investigate if there was any internal damage; there was very slight bending of the dowels, which indicates that the connections may have remained mostly elastic during the TBRBF tests as well as the bare frame tests. Throughout testing, the rotation of the connections was monitored by linear variable displacement transducers (LVDTs); they recorded a maximum rotation of 0.036 radians during the testing series.

4 CONCLUSIONS

Six beam-column joint specimens were tested which achieved a rotation of 0.11 rad. This large rotation shows that the connections behave in a ductile manner, a good characteristic of an element in a LFRS. The MPL material did not experience any perpendicular to grain splitting; this eliminates the need for costly joint reinforcement and confirms the hypothesis that the cross-grain layers would behave as self-reinforcing by providing additional stiffness in the perpendicular-to-grain direction. Additionally, the 25 mm gap helped avoid crushing of the timber by preventing contact between the beam end and column face. The bending moment that the joint was able to resist was proportional to the number of dowels in the beam. The results of these tests showed that the existing

https://doi.org/10.52202/069179-0265

methods for connection design are applicable for this type of connection and result in a ductile response.

After the connection tests, a series of timber frame tests were completed including four tests with a TBRB and five tests with the bare frame. All four TBRBFs achieved similar forces and drifts in both tension and compression; the TBRBs consistently failed during the compression portion of the 100%Δ_m step of the loading protocol. The failure mode was weak axis buckling of the steel core near the end of the yielding zone. The increasing amplitude of the waves eventually caused the MPP casing to split along its length. The TBRB improved the performance of the subassembly by improving the hysteretic energy capabilities by 4.0 to 8.6 times and increasing the lateral load capacity by a factor of 3.0 to 3.8. The ductility of the TBRBF was evaluated using two methods and was found to be comparable with other timber frames using conventional BRBs and double the ductility of conventional timber braced frames.

The same frame was used for all nine tests with no visible damage to the connections. This demonstrates the resilience of this TBRBF system where the TBRB can be removed and replaced following a seismic event, without the need to replace the bare timber frame. Further testing including full-scale dynamic tests is suggested to confirm the findings of this study.

ACKNOWLEDGEMENT

The authors acknowledge the financial support provided by Wood Innovations, USDA Grant 20-DG-11046000-615, the donation of materials by Freres Lumber Co., Inc., and the in-kind CNC fabrication assistance provided by the Timberlab. The authors acknowledge the assistance of M. Bryant, D. Tran, I. Dangol, D. Briggs, S. Neupane and S. Shrestha of the University of Utah for their assistance in carrying out the experiments.

REFERENCES

[1] Morrell I., Soti R., Miyamoto B. and Sinha A.: Experimental Investigation of Base Conditions Affecting Seismic Performance of Mass Plywood Panel Shear Walls. *J. Struct. Eng*. 146(8), 2020.

[2] Lo Ricco M., Rammer D.R., Amini M.O., Ghorbanpoor A., Shiling P. and Zimmerman, R.B.: Equivalent lateral force procedure for a building with a self-centering rocking story of cross-laminated timber (CLT) walls." *Proceedings of the World Conference on Timber Engineering 2020*, 2021. Santiago, Chile.

[3] Pei, S., van de Lindt, J.W., Barbosa, A.R., Berman, J.W., McDonnell, E., Dolan, J.D., Blomgren, H.-E., Zimmerman, R.B., Huang, D., and Wichman, S.: Experimental seismic response of a resilient 2-story mass-timber building with post-tensioned rocking walls. *J. Struct. Eng*., 145(11): 04019120, 2019.

[4] van de Lindt J., Amini, O.M., Rammer D.; Line P.; Pei S., Popovski M.: Determination of seismic performance factors for cross-laminated timber shear walls based on FEMA P695 methodology. *General Technical Report FPL-GTR-281*, 2022.

[5] Ganey R., Berman J., Akbas T., Loftus S., Dolan J.D., Sause R., Ricles J., Pei S., van de Lindt J. and Blomgren H.-E.: Experimental investigation of self-centering cross-laminated timber walls. *Journal of Structural Engineering,* 2017.

[6] Busch, A., Zimmerman, R.B., Pei, S., McDonnell, E., Line, P., and Huang, D.: Prescriptive seismic design procedure for post-tensioned mass timber rocking walls. *Journal of Structural Engineering*, 148(3): 04021289, 2022.

[7] Cao J., Xiong H. and Cui Y.: Seismic performance analysis of timber frames based on a calibrated simplified model. *Journal of Building Engineering* 46, 2021.

[8] Popovski M., Prion H. G.L. and Karacabeyli E.: Shake table tests on single-storey braced timber frames. *Canadian Journal of Civil Engineering* 30:1089-1100, 2003.

[9] Murphy, C., Pantelides, C.P., Blomgren, H., Rammer, D.: Development of timber buckling restrained brace for mass timber-braced frames. *Journal of Structural Engineering*, 147(5):04021050, 2021.

[10] AISC: Seismic Provisions for Structural Steel Buildings. ANSI/AISC 341-16, Chicago, American Institute of Steel Construction, 2016.

[11] Takeuchi T., Terazawa Y., Komuro S., Kurata T. and Sitler B.: Performance and failure modes of mass timber buckling-restrained braces under cyclic loading. *Engineering Structures* 266, 2022.

[12] Dong W., Li M., Lee C., MacRae G., and Abu A.: Experimental testing of full-scale glulam frames with buckling restrained braces. *Engineering Structures* 222, 2020.

[13] Rebouças A.S., Mehdipour Z. Branco J.M. and Lourenço P.B.: Ductile Moment-Resisting Timber Connections: A Review. *Buildings*. 12(240), 2022.

[14] Popovski M., Prion H. G.L., and Karacabeyli E.: Seismic performance of connections in heavy timber construction. *Canadian Journal of Civil Engineering* 29:389-399, 2001.

[15] Ogrizovic J., Wanninger F. and Frangi, A.: Experimental and analytical analysis of moment-resisting connections with glued-in rods. *Engineering Structures.* 145: 322-332, 2017.

[16] Steiger R., Serrano E., Stepinac M., Rajcic V., O'Niell C., McPolin D. and Widmann, R.: Strengthening of timber structures with glued-in rods. *Construction and Building Materials*, 97:90-105, 2015.

[17] Dong, W., Li, M., He, M., Li, Z.: Experimental testing and analytical modeling of glulam moment connections with self-drilling dowels. *Journal of Structural Engineering*, 147(5): 04021047, 2021.

[18] Bouchaïr, A., Racher, P., Bocquet, J.F.: Analysis of dowelled timber to timber moment-resisting joints. *Materials and Structures*, 40:1127-1141, 2007.

[19] APA (The Engineered Wood Association): Freres Mass Ply Panels (MPP), and Mass Ply Lam (MPL) Beams and Columns, Freres Lumber Co.. *Inc. PR-L325*, 2022
[20] Williamson E., Pantelides C. P., Blomgren H.-E. and Rammer D.: Performance of beam-column connections with Mass Ply Lam and steel dowels under cyclic loads. *Journal of Structural Engineering,* 149(6):04023057, 2023.
[21] AWC (American Wood Council): National Design Specification for Wood Construction, 2018.
[22] AWC (American Wood Council): Technical Report 12: General Dowel Equations for Calculating Lateral Connection Values with Appendix A, 2018.
[23] Fan, X., Zhang, S., Qu, W.: Load-carrying behaviour of dowel-type timber connections with slotted-in steel plates. *Applied Mechanics and Materials*, 94-96: 43-47, 2011.
[24] ASTM: Standard Test Methods for Cyclic (Reversed) Load Test for Shear Resistance of Vertical Elements of the Lateral Force Resisting System for Buildings. *ASTM E2126*, 2011
[25] Yasumura M. and Kwai N.: Estimating seismic performance of wood-frame structures." *Proceedings of the 5th World Conference on Timber Engineering*, 1998. Presses Polytechniques et Universitaires Romandes.
[26] Muñoz W., Mohammad M., Salenikovich A. and Quenneville P.: Determination of yield point and ductility of timber assemblies: in search for a harmonized approach. *Engineered Wood Products Association*, 2008.
[27] Xiong H. and Liu Y.: Experimental study of the lateral resistance of bolted glulam timber post and beam structural systems. *Journal of Structural Engineering*, 142(4), 2014.

https://doi.org/10.52202/069179-0265